



Cite this: *Catal. Sci. Technol.*, 2025, 15, 7414

E-Selective partial transfer hydrogenation of internal acetylenes enabled by water-promoted Fe(CO)₅ catalysis

Manisha, Lalit Negi, Deepali Ahluwalia, Akansha Soni, Aarti Peswani and Raj K. Joshi

Hydrogen transfer *via* water splitting with an iron catalyst presents challenging opportunities. In this note, we have introduced a novel approach for the transfer hydrogenation of internal acetylenes, yielding highly chemo- and stereo-selective *E*-stilbenes using an earth-abundant iron-catalyst and water as a green hydrogen source. The established protocol showed a broad applicability towards various directing acetylenes, while maintaining high tolerance for functional groups. The method avoids the common issue of isomerization and over-reduction to alkanes. Interestingly, the method is cost-effective for the synthesis of deuterated substrates too. The iron-hydride formed as an intermediate is responsible for the semi-hydrogenation of alkynes, and it is validated through DFT calculations.

Received 16th August 2025,
Accepted 18th October 2025

DOI: 10.1039/d5cy01004g

rsc.li/catalysis

Introduction

Chemo- and stereo-selective transfer hydrogenation (TH) is valued in synthetic chemistry for its efficiency in modifying functional groups with control. Among these, the stereo-selective hydrogenation of acetylene to *E*-stilbene is a unique and vital reaction, offering efficient synthesis of specific *trans*-alkene frameworks.¹ A significant challenge in this approach is to achieve precise configurations while preventing over-reduction and isomerization. Stilbenes, with well-defined configurations (either *E* or *Z*), serve as versatile intermediates for further transformations, promoting developments in materials science, agrochemicals, and drugs.² Fig. 1 showcases some important stilbenes, demonstrating the adaptability of this reduction chemistry.

Traditionally, alkynes were reduced *via* Wilkinson's³ and Lindlar's (Pd-BaSO₄) catalysts⁴ for *Z*-alkenes, and the Birch reduction for *E*-alkenes.⁵ However, these methods often limit functional group endurance and chemo-selectivity. Noble metals, such as Pd,⁶ Ru,⁷ and Ir,⁸ are extensively explored, but sustainable synthetic approaches are in demand for the future; therefore, earth-abundant transition metals like Mn,⁹ Co,¹⁰ Ni,¹¹ and Cu¹² are becoming important.

Emanating from this, iron catalysis has grown significantly, as it allowed expansive transformations, offering high reactivity, selectivity, and unique mechanistic pathways.¹³ This versatility emphasizes the vital role of iron in developing cutting-edge catalytic processes. In 1989,

Bianchini *et al.* reported iron-catalyzed partial hydrogenation of acetylenes.^{14a} Afterwards, Milstein,^{14b} Kirchner,^{14c} and Khusnutdinova^{14d} have described similar chemistry using different iron complexes. In 2012, Beller *et al.*^{15a} utilized HCOOH, a surrogate for hydrogen, using an iron-complex, following this, transfer hydrogenation using an iron catalyst extended its significance.^{15b-e} Fe(0) complexes, *i.e.*, Fe₂(CO)₉ with monodentate phosphines produced *Z/E*-stilbenes^{15f} by reduction of internal alkynes; here, (EtO)₃SiH was used as a H-donor. Although these procedures effectively produced stereo-selective alkenes, but they typically worked under an inert atmosphere and involved a multi-step method for synthesis. An overview of iron-catalyzed semi-hydrogenation of alkynes is shown in Scheme 1.

However, facile protocols utilizing an aqueous catalytic system are highly desirable, where water serves as a green solvent and active reactant, enabling unique, eco-friendly transformations.^{2e,13b} Shirakawa and Hayashi were the first to report the use of water, as a hydrogen surrogate for the partial

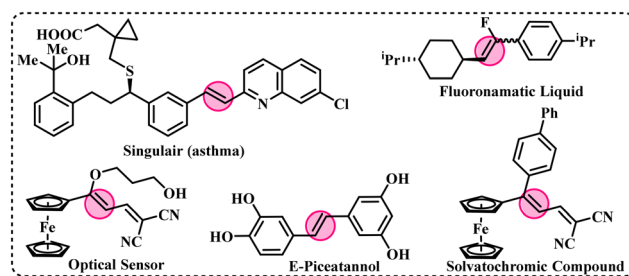
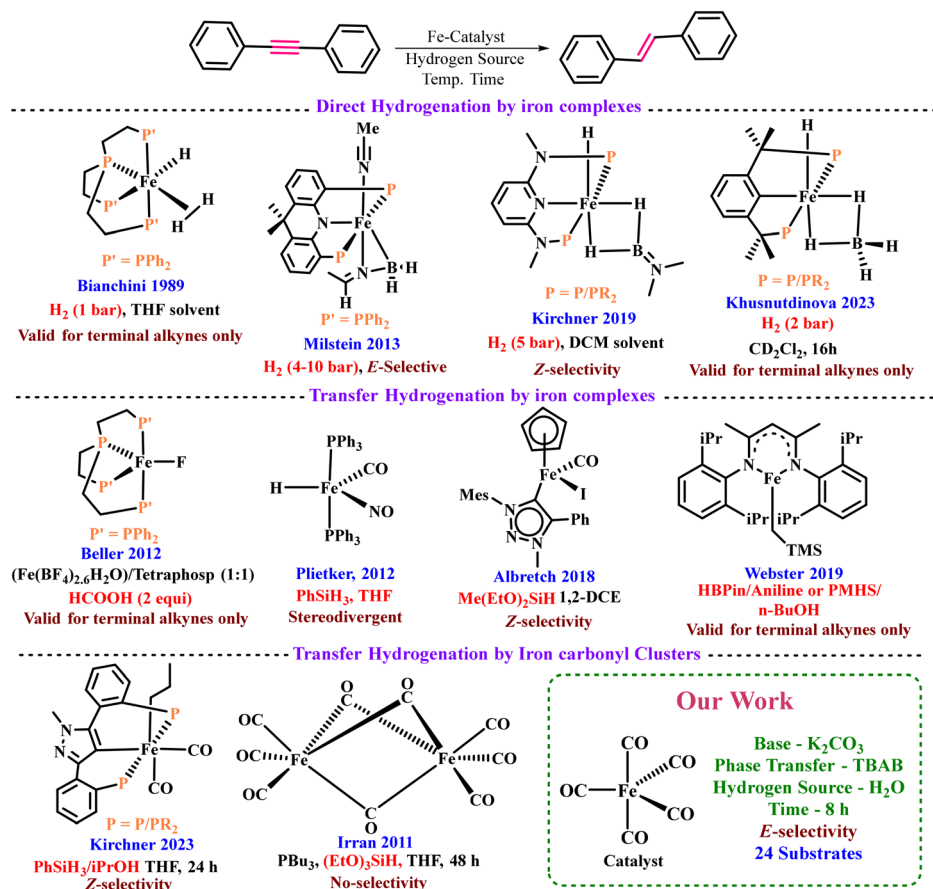


Fig. 1 Stilbenes supporting the need for selective synthetic approaches and their diversity.

Department of chemistry, Malaviya National Institute of Technology Jaipur, JLN Marg, Jaipur-302017, Rajasthan, India. E-mail: rkjoshi.chy@mnit.ac.in



Scheme 1 Comparison between the previous and present work.

transfer hydrogenation of alkynes¹⁶ with a Pd-catalyst. Subsequent studies also explored transfer hydrogenation of acetylene with Pd¹⁷ and Co,¹⁸ Cu,¹⁹ and Ni²⁰ with water. Here, the catalytic system frequently depends on auxiliary reductant-supported bimetallic frameworks (*e.g.*, Zn, Mn).

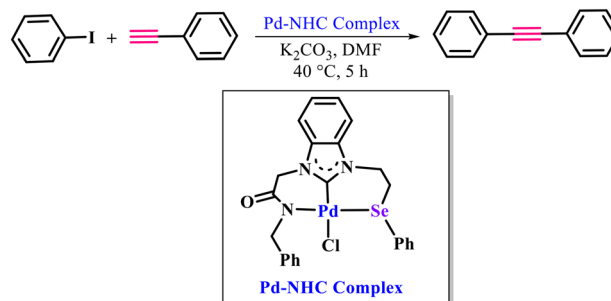
Despite these advancements, water has not yet been investigated as a surrogate of hydrogen for iron catalysis in conventional organic reactions. In contrast, iron catalysis in water has only been explored electrochemically, and these studies demonstrate its potential to generate hydrogen through water electroreduction.²¹ This indicates a significant opportunity to explore water-based iron catalysis for green synthesis.

$Fe(CO)_5$ is a versatile catalyst that facilitates diverse reactions with remarkable efficiency.²² Recently, $Fe(CO)_5$ was used for the transfer hydrogenation of chalcones with water as a hydrogen donor.²³ This result motivates us to investigate further the hydrogenation potential of $Fe(CO)_5$ to reduce alkynes. Herein, we have successfully developed a stereo- and chemo-selective partial transfer hydrogenation of internal alkynes utilizing iron pentacarbonyl as a catalyst in the presence of base K_2CO_3 and water as a hydrogen surrogate. Furthermore, this approach is also applicable for synthesizing deuterated stilbene, a valuable pharmaceutical resembling Austedo (deutetrabenazine), the first FDA-approved deuterated drug for treating Huntington's disease.²⁴

Experimental section

Synthesis of internal alkynes

To a mixture of aryl bromide/iodide (1.0 mmol), K_2CO_3 (2.0 mmol), acetylene (1.2 mmol), and *N,N*-dimethylacetamide (DMA, 1.5 mL), the NHC-Pd(II) full pincer catalyst (12 mg, 0.02 mmol) was added (SI, ref. 6). The reaction mixture was heated at 40 °C for 5 h with constant stirring. The resulting reaction mixture was allowed to cool down at room temperature, and the organic layer was separated by solvent extraction in ethyl acetate and water.



After drying the organic layer on sodium sulphate and concentrating over a rotary evaporator, the desired product

was separated by column chromatography using hexane/ethyl acetate as an eluent.

General procedure for catalytic semi-hydrogenation of acetylenes

In a 15 mL reaction tube equipped with a magnetic stirrer, a mixture of 1.0 mmol of internal acetylene, 0.5 mmol of potassium carbonate (K_2CO_3) base, 0.4 mmol of TBAB, and 20.0 mol% of $Fe(CO)_5$ was stirred at 110 °C for 8 h in aqueous medium (DI water). Upon completion, the mixture was cooled down to room temperature and transferred to a separating funnel for solvent extraction with ethyl acetate and water. Then, it was dried over anhydrous sodium sulfate, filtered, and concentrated under reduced pressure. The crude product was purified by column chromatography using hexane/ethyl acetate to get the pure product as a white solid. The purified product was characterized by 1H and $^{13}C\{H\}$ -NMR spectroscopy.

Results and discussion

Screening of parameters

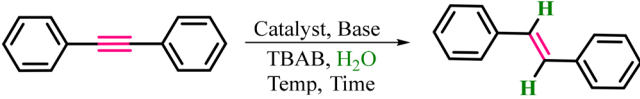
Encouraged by the catalytic potential of $Fe(CO)_5$ for water-assisted hydrogen generation,²³ we employed the same approach to investigate the transfer hydrogenation of acetylenes. For this, biphenyl acetylene was chosen as a key substrate, and the elementary conditions of the optimization have been summarized in Table 1. The initial trial reaction of

biphenyl acetylene in the presence of $Fe(CO)_5$ with base, K_2CO_3 , and water as a solvent at 110 °C for 12 h produced biphenyl alkene with 59% yield (Table 1, entry 1). However, no further reduction of the alkene to alkane was recorded when the reaction was allowed to run for 24 h under the same conditions. Gratifyingly, a significant improvement in the yield of the product was noticed when a biphasic catalyst, TBAB, was introduced. Here, we find that adding TBAB, a biphasic reagent, promotes the reaction, perhaps by improving the solubility of the catalyst. TBAI and TBAF biphasic reagents also facilitated the reaction, but TBAB showed superior efficiency due to its ideal balance of nucleophilicity.

The catalytic potential of other iron-based clusters, $Fe_2(CO)_9$, $Fe_3(CO)_{12}$, and $Fe_3Se_2(CO)_{12}$, was investigated, but none of them was found suitable (Table 1, entries 2–4). The thermal condition, presence of mild base, and low catalytic potential of these clusters may be the reason.

Moreover, no product was obtained under catalyst-free and base-free conditions, which indicates the prime requisites of the base and catalyst for the present reaction (Table 1, entries 5–6). Next, the optimization of the amount of iron catalyst was conducted, and 0.2 equivalent of iron catalyst was found to be ideal for the significant transformation, while reducing the amount of iron catalyst (10 mol%) drastically reduced the transformation, while increasing the amount to 30 mol% did not considerably impact on the yield (Table 1, entries 7–9). The base

Table 1 Optimization of reaction conditions



Sr. no.	Catalyst (mol%)	Base (mmol)	Temp (°C)	Time (h)	Yield ^a (%)
1.	$Fe(CO)_5$ (20)	K_2CO_3 (1)	110	12	59 ^b
2.	$Fe_2(CO)_9$ (20)	K_2CO_3 (1)	110	12	n.d
3.	$Fe_3(CO)_{12}$ (20)	K_2CO_3 (1)	110	12	n.d
4.	$Fe_3Se_2(CO)_{12}$ (20)	K_2CO_3 (1)	110	12	n.d
5.	$Fe(CO)_5$ (20)	—	110	12	n.d
6.	—	K_2CO_3 (1)	110	12	n.d
7.	$Fe(CO)_5$ (10)	K_2CO_3 (1)	110	12	47
8.	$Fe(CO)_5$ (20)	K_2CO_3 (1)	110	12	82
9.	$Fe(CO)_5$ (30)	K_2CO_3 (1)	110	12	84
10.	$Fe(CO)_5$ (20)	K_2CO_3 (0.25)	110	12	41
11.	$Fe(CO)_5$ (20)	K_2CO_3 (0.50)	110	12	82
12.	$Fe(CO)_5$ (20)	K_2CO_3 (0.75)	110	12	83
13.	$Fe(CO)_5$ (20)	K_2CO_3 (0.5)	RT	12	n.d
14.	$Fe(CO)_5$ (20)	K_2CO_3 (0.5)	50	12	Trace
15.	$Fe(CO)_5$ (20)	K_2CO_3 (0.5)	80	12	47
16.	$Fe(CO)_5$ (30)	K_2CO_3 (0.5)	130	12	83
17.	$Fe(CO)_5$ (20)	K_2CO_3 (0.5)	110	4	28
18.	$Fe(CO)_5$ (20)	K_2CO_3 (0.5)	110	6	46
19.	$Fe(CO)_5$ (20)	K_2CO_3 (0.5)	110	8	81
20.	$Fe(CO)_5$ (20)	K_2CO_3 (0.5)	110	10	82
21.	$Fe(CO)_5$ (20)	K_2CO_3 (0.5)	110	10	39 ^c
22.	$Fe(CO)_5$ (20)	K_2CO_3 (0.5)	110	10	29 ^d

Reaction conditions: diphenyl acetylene (178 mg, 1 mmol), TBAB (80 mg, 0.40 mmol), H_2O (2 mL, DI). ^a Isolated yield. ^b Without TBAB. ^c In the presence of IPA instead of water. ^d In the presence of Et_3SiH in toluene instead of water.

optimization showed a significant and decent feasibility of the reaction with various bases, including K_3PO_4 , $tBuOK$, and Cs_2CO_3 ; however, the best result was recorded with K_2CO_3 . It was also noted that 0.5 mmol of K_2CO_3 produced significant transformations (Table 1, entries 10–12). During the temperature optimization, the formation of the product commenced at 50 °C, it kept on increasing with the gradual rise in temperature, and finally it became constant at 110 °C (Table 1, entries 13–16). Furthermore, the duration of reaction was optimized, and it was quite encouraging to get the desired product in just 8 hours (Table 1, entries 17–20). Surprisingly, the reaction was found less effective with alcohol (*i.e.*, isopropyl alcohol) and silanes despite their higher potential as hydrogen donors than water; only 39% and 29% yields were obtained, respectively (Table 1, entries 21–22). Therefore, it may be concluded that for the *E*-stereoselective transfer semi-hydrogenation of alkynes, the iron-catalyst $Fe(CO)_5$ (0.20 equiv.), K_2CO_3 (0.5 equiv.), TBAB (0.4 equiv.), and water, as a hydrogen source and reaction medium, at 110 °C for 8 h served the best fitted conditions for efficient transformation (Table 1, entry 19).

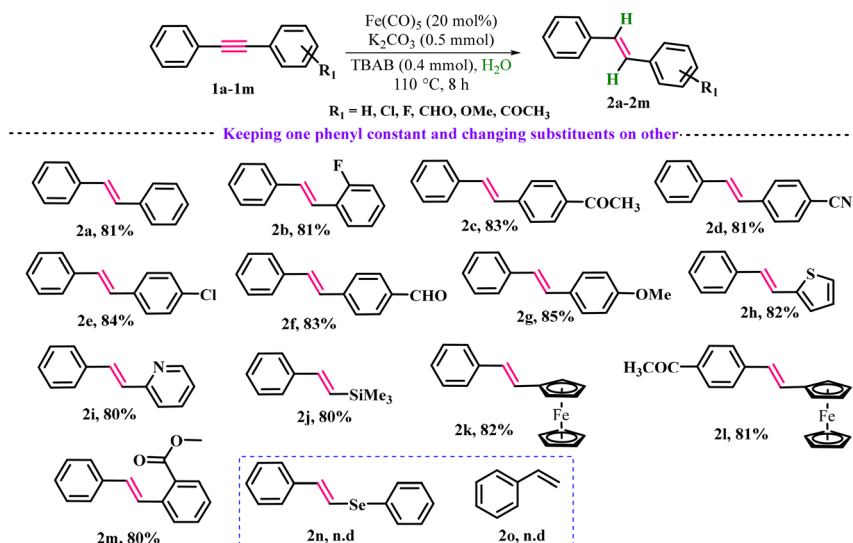
Substrate scope

After getting the best optimized conditions for the present reaction, the general substrate scope towards various internal alkynes was evaluated, as depicted in Scheme 2. First, alkynes bearing substituents on one of the phenyl ring were investigated. Diphenylacetylene (**2a**) was partially reduced under the optimized conditions to produce 81% of diphenylalkene. Moreover, the *ortho*-fluoro (**2b**) and *para*-cyanophenyl substitutions (**2d**) also reacted in the same manner and gave the same yields of the desired alkenes. However, a marginally improved transformation of 83% was recorded for the *para*-substituted acetyl and carbaldehyde diphenylacetylenes (**2c** and **2f**). Nevertheless, the yield of the

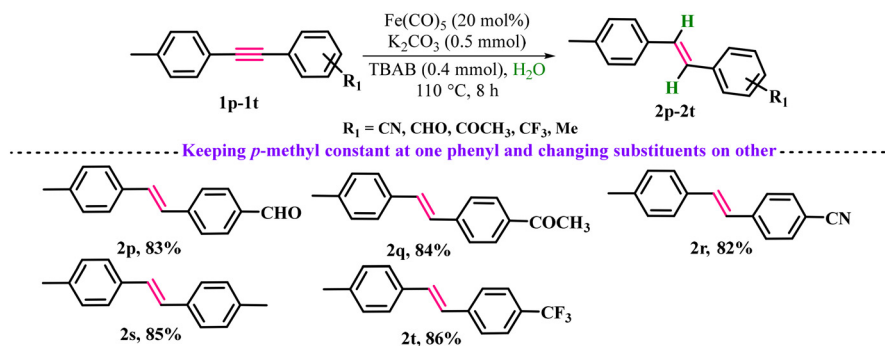
semi-hydrogenated product was further increased to 84% for the *p*-chloro (**2e**) and 85% for *p*-methoxy (**2g**) substituted biphenyl acetylenes. Notably, there was no evidence of dehalogenation; moreover, the carbonyl and nitrile groups were also preserved under the same conditions, underscoring the remarkable chemo-selectivity of the present reaction. Moreover, the transformation was not significantly affected by the nature of the electron rich or electron poor group attached on the benzene ring of acetylenes. Moving further, the scope of the reaction was further extended to heterocyclic-substituted internal alkynes.

The thiophene and pyridine substituted alkynes were found well tolerated for the reaction, furnishing the corresponding alkenes with excellent stereoselectivity in 82% and 80% yields, respectively (**2h** and **2i**). It is worth mentioning that an alkaline sensitive alkene (1-phenyl-2-(trimethylsilyl) acetylene) was also well tolerated under the established reaction parameters and yielded 80% of the desired alkene product (**2j**). Furthermore, the scope of the reaction was also investigated for alkynes bearing an organometallic ferrocene group *i.e.* ferrocenyl-phenyl acetylene (**2k**) and *para*-acetyl substituted ferrocenyl-phenyl acetylenes (**2l**); both were found highly effective and successfully transformed into the reduced alkenes with 82% and 81% conversion, respectively. An ester group bearing alkyne *i.e.* methyl 2-(phenylethynyl)benzoate (**2m**) was also explored, the transformation proceeded very smoothly without affecting the ester functionality with 80% yield of the desired alkene; this indicates the potential of the present method for late-stage functionalization of ester-containing molecules. However, phenyl(phenylethynyl)silane was failed to produce (*E*)-phenyl(styryl)silane (**2n**). Moreover, terminal acetylenes were also found inactive for the present reaction protocols, and even a trace of styrene was not detected (**2o**).

Next, the scope of the reaction was investigated for alkynes consisting substitutions on both phenyl rings;



Scheme 2 Scope for biphenyl acetylene bearing variant substituents.



Scheme 3 Substrate variability in biphenyl acetylenes substituted on both sides.

keeping the *p*-methyl phenyl constant at one of the terminals, the functional variations were made at the phenyl ring present at other terminals of alkynes (Scheme 3, entries **2p–2t**). *Para*-carbaldehyde, *para*-acetyl, *para*-cyano, and *para*-trifluoromethyl groups present at one of the terminals of acetylene were checked for the iron-catalyzed reduction with water as a hydrogen surrogate; all functional groups were found well tolerated and all alkyne derivatives gave good yields of the desired reduced alkenes in the range of 82% to 86%.

Besides this, the scope of the reaction for reducing isolated diacetylenes, 1,4-bis(phenylethynyl)benzene, was investigated and depicted in Scheme 4. Here, likewise the mono acetylenes, both the C≡C triple bonds were partially reduced into alkene, and the formation of 79% 1,4-distyrybenzene (**2u**) was obtained. Moreover, the same product was also obtained by reducing 1-(phenylethynyl)-4-styrylbenzene, where the triple bond was exclusively reduced and the double bond remained intact. This indicates the selective reduction of the present method towards alkynes. The method was reasonably valid for varieties of internal acetylenes and produced good yields of the products

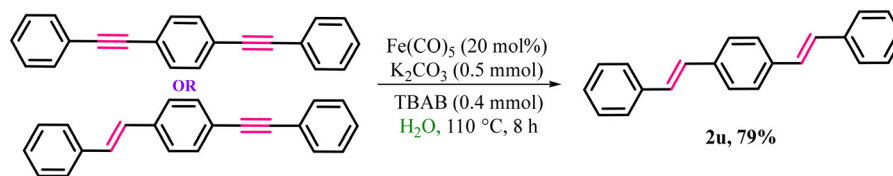
irrespective of the nature of the functional group present on the phenyl ring. Hence, it demonstrates excellent functional group tolerance for the semi-hydrogenation process, particularly towards halides such as F, Cl, and CF₃ without any dehalogenation product.

Deuterium labeling experiment

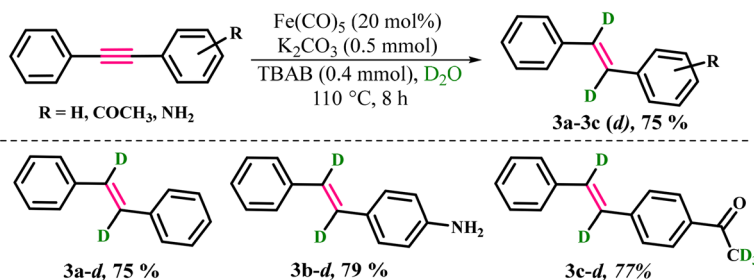
To confirm that water is the only source of hydrogen for the reduction of alkyne to alkene in the present reaction, isotopic labelling experiments were conducted and D₂O was used as a solvent (Scheme 5), and the obtained results were validated by NMR spectroscopy (SI, Schemes S2 and S3).

A 75% yield of deuterated biphenyl alkene was recorded under the established reaction conditions just by replacing H₂O with D₂O; this confirmed that water is the only source of hydrogen for the reduction.

Deuterium incorporation was further examined using substrates containing acetyl and amine functionalities and significant reduction of alkyne with deuterium was recorded. Moreover, unlike amine substrates, which remain unaffected, deuterium incorporation occurred at the methyl



Scheme 4 Chemo-selectivity among alkene and alkyne groups.



Scheme 5 Evaluation of deuterium-labeled substrates.

position of the acetyl group, indicating its relative sensitivity²⁵ (Scheme 5, entries 3a–3c (d)). The developed protocol for synthesizing deuterium-labelled compounds provides a practical tool for mechanistic investigations and kinetic isotope effect studies.

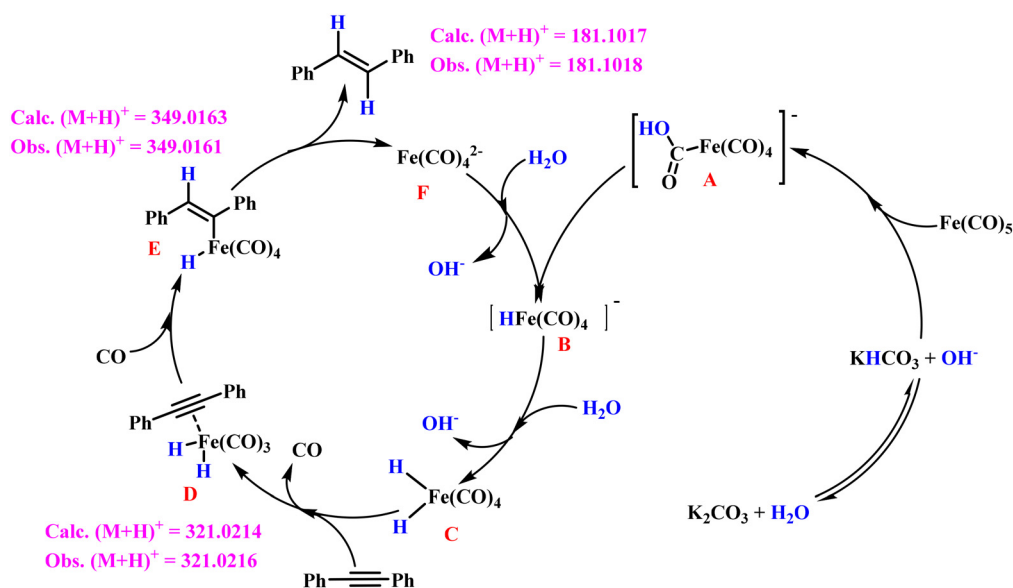
Plausible mechanism

Based on our experimental observations and previous literature, we have proposed a plausible mechanism for the present reaction (Scheme 6). Reactions with radical scavengers (TEMPO & BHT) confirmed that the reaction does not follow the radical route. Deuterium labelling studies confirmed the role of water as a source of hydrogen *via* the coordination of alkyne and Fe(CO)₅, followed by transfer hydrogenation (SI, Schemes S2 and S3).

Moreover, the HRMS fragments hint at important intermediates of the transformations (SI, Fig. S22–S24), which were further confirmed by DFT calculations. The preliminary DFT optimizations were carried out employing 6-311G** and LANL2DZ sets using water as a solvent. The IEFPCM model was incorporated as it propounded the best available boundary conditions for the apparent surface charge isotropic dielectric continuum solvation model, combining robustness concerning outlying charge effects and computational efficiency [SI, computation details].

The reaction was carried out in water, which is also the source of hydrogen, hence, the dielectric constant of water ($\epsilon = 78.35530$) was taken into account. Scheme 6 and Fig. 2 describe the plausible mechanism and energy profile, respectively. The reaction was initiated with the activation of iron (0) carbonyl upon the addition of K₂CO₃ and water.^{23,26a} This leads to the formation of an active intermediate **A**, bearing a negative charge on the complex, and the relative Gibbs free energy of **A** was found to be -0.057 kcal mol⁻¹.

The reaction may proceed *via* a transition state, TS_{AB}, detected by the unique imaginary frequency, having relative $\Delta G = 3.22$ kcal mol⁻¹. Herein, the C–O–H bond of the carboxylic group is particularly focused. As per observation, the C–O bond was nearly 1.27 Å and the O–H bond distance was 1.67 Å, which must be close to the reported 0.96 Å. The shortening of C–O bond and lengthening of O–H bond pointed towards the hydrogen transfer from the carboxyl group to the central metal iron, and accompanied by the release of carbon dioxide to form intermediate **B**, which has a relative ΔG value of 0.042 kcal mol⁻¹. Moving further, water plays a pivotal role as a source for another H-atom to be attached with iron catalyst, which resulted in intermediate **C**. The intermediate **D**, formed *via* the coordination of C≡C bonds of biphenyl acetylene with intermediate (**C**), which shows the $\Delta G = 1.57$ kcal mol⁻¹, and also confirmed by the HRMS analysis²⁶ (SI, Fig. S22). Next to this, another transition state TS_{DE} was detected, where the transfer of H from iron-complex to the acetylene occurred and a sudden energy rise from intermediate **D** was observed here ($\Delta G = 11.63$ kcal mol⁻¹). This step is the pivot and depicts the first transfer hydrogenation to reduce the acetylene; at this stage, the distance between the second hydride ligand and the acetylene carbon was nearly 1.54 Å. The triple bond was expected to be reduced into a double bond as the H-transfer takes place, and HFe(CO)₄ shifted to the second carbon of *E*-stilbene,^{14c} and it was marked as intermediate **E**²⁶ (SI, Fig. S23). Thereafter, the second hydride transfer occurred from iron-to the second carbon of alkyne, and formed the stilbene–iron complex (intermediate **F**). The relative energy of this intermediate was found slightly higher, owing to the weakening of the iron complex interaction with *E*-stilbene. Thus, the rise in energy of this intermediate may be attributed to the unstable tetra-coordinated system. Water as a solvent can play a key role in stabilizing this complex. As



Scheme 6 Plausible mechanism for the semi-hydrogenation of acetylene.

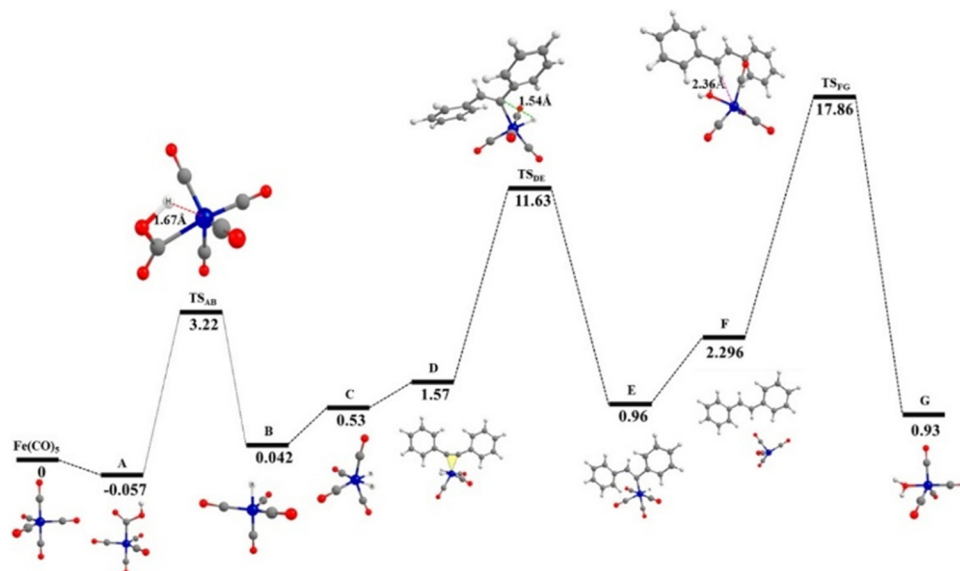


Fig. 2 Free energy profile diagram depicting precatalytic activation. Relative free energies of complexes are reported in kcal mol⁻¹.

depicted in TS_{FG}, water coordinates with the iron-catalyst, yielding a penta-coordinated metal complex, with $\Delta G = 17.86$ kcal mol⁻¹. This transition state is highly unstable, the product (*E*-stilbene) may be withdrawn at this stage. The distance between the iron catalyst and the product was found to be nearly 2.36 Å. This may lead to easy removal of the product, leading to the formation of intermediate G. The catalytic cycle again repeats itself as the hydroxyl ion gets removed, and intermediate B is formed again to continue the catalytic cycle. This pathway highlights the crucial roles of water and base in both catalyst activation and regeneration, enabling efficient and stereoselective hydrogenation.

Conclusion

This study increased the understanding of the Fe(CO)₅-based catalytic system for the hydrogenation of alkynes under mild conditions. Water, a green solvent, was utilized as a hydrogen surrogate, which is rare to observe, especially with highly economical iron metal. A wide range of internal alkynes, irrespective of attached functional groups, were smoothly utilized for efficient semi-hydrogenation to yield *E*-stereoselective stilbenes. Additionally, the method facilitates synthesis of 1,2-dideuterioalkenes from inexpensive deuterium oxide. Density functional theory (DFT) calculations provide insight into the proposed reaction mechanism.

Conflicts of interest

There are no conflicts to declare.

Data availability

The data supporting this article have been included as part of the supporting information (SI).

Supplementary information: experimental, and computational information, NMR, and HRMS characterization of the products are available in the SI. See DOI: <https://doi.org/10.1039/d5cy01004g>.

Acknowledgements

Raj K. Joshi thanks CSIR (01(2996)/19/EMR-II) for financial assistance. Manisha & Akansha Soni thank the CSIR-UGC for a research fellowship. Lalit Negi & Aarti Peswani thank MNIT Jaipur for research fellowships.

Notes and references

- (a) K. C. K. Swamy, A. S. Reddy, K. Sandeep and A. Kalyani, *Tetrahedron Lett.*, 2018, **59**, 419–429; (b) B. J. Gregori, M.-O. W. S. Schmotz and A. J. V. Wangelin, *ChemCatChem*, 2022, **14**, e202200886; (c) R. Kusy and K. Grell, *Chem. Rev.*, 2025, **125**, 4397–4527.
- (a) Z. A. Khan, A. Iqbal and S. A. Shahzad, *Mol. Diversity*, 2017, **21**, 483–509; (b) T. Teka, L. Zhang, X. Ge, Y. Li, L. Han and X. Yan, *Phytochemistry*, 2022, **197**, 113128; (c) K. F. Filmon, L. Delaude, A. Demonceau and A. F. Noels, *Coord. Chem. Rev.*, 2004, **248**, 2323–2336; (d) L. Negi, A. Soni, M. Manisha, C. Sharma and R. K. Joshi, *J. Organomet. Chem.*, 2023, **1001**, 122847; (e) L. Negi, A. Soni, D. Sharma, M. Manisha and R. K. Joshi, *J. Org. Chem.*, 2025, **90**, 2567–2576; (f) A. Soni, L. Negi, C. Sharma, A. K. Srivastava and R. K. Joshi, Oxidative Coupling of Primary Benzamide with Alkenes via o-CH Activation Mediated by Cu(II)/Ru(II), *J. Org. Chem.*, 2024, **89**(23), 17752–17760.
- J. A. Osborn, F. H. Jardine, J. F. Young and G. Wilkinson, *J. Chem. Soc. A*, 1966, (0), 1711–1732.
- H. Lindlar and R. Dubuis, *Org. Synth.*, 1966, **46**, 89–92.
- A. J. Birch, *J. Chem. Soc.*, 1944, 430–436.

- 6 (a) A. Monfredini, V. Santacroce, L. Marchiò, R. Maggi, F. Bigi, G. Maestri and M. Malacria, *ACS Sustainable Chem. Eng.*, 2017, **5**, 8205–8212; (b) F. Luo, C. Pan, W. Wang, Z. Ye and J. Cheng, *Tetrahedron*, 2010, **66**, 1399–1403.
- 7 T. Schabel, C. Belger and B. Plietker, *Org. Lett.*, 2013, **15**, 2858–2861.
- 8 K. Tani, A. Iseki and T. Yamagata, *Chem. Commun.*, 1999, 1821–1822.
- 9 R. A. Farrar-Tobar, S. Weber, Z. Csendes, A. Ammaturo, S. Fleissner, H. Hoffmann, L. F. Veiros and K. Kirchner, *ACS Catal.*, 2022, **12**, 2253–2260.
- 10 D. M. Sharma, C. Gouda, R. G. Gonnade and B. Punji, *Catal. Sci. Technol.*, 2022, **12**, 1843–1849.
- 11 N. O. Thiel, B. Kaewmee, T. T. Ngoc and J. F. Teichert, *Chem. – Eur. J.*, 2019, **26**, 1597–1603.
- 12 K. Semba, T. Fujihara, T. Xu, J. Terao and Y. Tsujia, *Adv. Synth. Catal.*, 2012, **354**, 1542–1550.
- 13 (a) C. Sharma, A. K. Srivastava, A. Soni, S. Kumari and R. K. Joshi, *RSC Adv.*, 2020, **10**, 32516–32521; (b) V. Tomar, D. Sharma, P. Kumar, D. Sharma, T. Singh, M. Nemiwal and R. K. Joshi, *Organometallics*, 2024, **43**, 2882–2894.
- 14 (a) C. Bianchini, A. Meli, M. Peruzzini, F. Vizza, F. Zanobini and P. Frediani, *Organometallics*, 1989, **8**, 2080–2082; (b) D. Srimani, Y. Diskin-Posner, Y. Ben-David and D. Milstein, *Angew. Chem., Int. Ed.*, 2013, **52**, 14131–14134; (c) N. Gorgas, J. Brüning, B. Stoger, S. Vanicek, M. Tilset, L. F. Veiros and K. Kirchner, *J. Am. Chem. Soc.*, 2019, **141**, 17452–17458; (d) D. K. Pandey, E. Khaskin, S. Pal, R. R. Fayzullin and J. R. Khusnutdinova, *ACS Catal.*, 2023, **1**, 375–381.
- 15 (a) G. Wienhofer, F. A. Westerhaus, R. V. Jagadeesh, K. Junge, H. Junge and M. Beller, *Chem. Commun.*, 2012, **48**, 4827–4829; (b) C. Belger and B. Plietker, *Chem. Commun.*, 2012, **48**, 5419–5421; (c) C. Johnson and M. Albrecht, *Catal. Sci. Technol.*, 2018, **8**, 2779–2783; (d) M. Espinal-Viguri, S. E. Neale, N. T. Coles, S. A. Macgregor and R. L. Webster, *J. Am. Chem. Soc.*, 2019, **141**, 572–582; (e) H. Schratzberger, B. Stoger, L. F. Veiros and K. Kirchner, *ACS Catal.*, 2023, **13**, 14012–14022; (f) S. Enthaler, M. Haberberger and E. Irran, *Chem. – Asian J.*, 2011, **6**, 1613–1623.
- 16 E. Shirakawa, H. Otsuka and T. Hayashi, *Chem. Commun.*, 2005, 5885–5886.
- 17 (a) S. P. Cummings, T. N. Le, G. E. Fernandez, L. G. Quiambao and B. J. Stokes, *J. Am. Chem. Soc.*, 2016, **138**, 6107–6110; (b) C.-Q. Zhao, Y.-G. Chen, H. Qiu, L. Wei, P. Fang and T.-S. Mei, *Org. Lett.*, 2019, **21**, 1412–1416.
- 18 K. Li, R. Khan, X. Zhang, Y. Gao, Y. Zhou, H. Tan, J. Chena and B. Fan, *Chem. Commun.*, 2019, **55**, 5663–5666.
- 19 X. Han, J. Hu, C. Chen, Y. Yuanb and Z. Shi, *Chem. Commun.*, 2019, **55**, 6922–6925.
- 20 K. Li, C. Yang, J. Chen, C. Pan, R. Fan, Y. Zhou, Y. Luo, D. Yang and B. Fan, *Asian J. Org. Chem.*, 2021, **10**, 1–5.
- 21 (a) Y.-W. Wang, Q. Wang and Y.-A. Qiu, *Nat. Commun.*, 2024, **15**, 2780; (b) H. Junge, N. Rockstroh, S. Fischer, A. Brückner, R. Ludwig, S. Lochbrunner, O. Kühn and M. Beller, *Inorganics*, 2017, **5**, 14.
- 22 (a) V. Tomar, P. Kumar, M. Nemiwal and R. K. Joshi, *Inorg. Chem. Commun.*, 2023, 111488; (b) M. Manisha, T. Jain, S. Kumari, L. Negi, S. Q. Raza and R. K. Joshi, *J. Organomet. Chem.*, 2023, **1001**, 122886.
- 23 M. Manisha, S. Kumari, D. Sharma, L. Negi and R. K. Joshi, *J. Org. Chem.*, 2024, **89**, 11983–11993.
- 24 A. Mullard, *Nat. Rev. Drug Discovery*, 2017, **16**, 305.
- 25 (a) K. I. Galkin, E. G. Gordeev and V. P. Ananikov, *Adv. Synth. Catal.*, 2021, **363**, 1368–1378; (b) X. Wang, Y.-F. Chen, L.-F. Niu and P.-F. Xu, *Org. Lett.*, 2009, **11**, 3310–3313.
- 26 (a) J.-J. Brunet, *Chem. Rev.*, 1990, **90**, 1041–1059; (b) T.-A. Mitsudo, H. Nakanishi, T. Inubushi, L. Morishima, Y. Watanabe and Y. Takegami, *J. Chem. Soc., Chem. Commun.*, 1976, 416–417; (c) T. Mitsudo, Y. Watanabe, H. Nakanishi, L. Morishima, T. Inubushi and Y. Takegami, *J. Chem. Soc., Dalton Trans.*, 1978, 1298–1304.